Journal of Power Sources 189 (2009) 72–80

Contents lists available at ScienceDirect

Journal of Power Sources

journal homepage: www.elsevier.com/locate/jpowsour

Surface film formation on a carbonaceous electrode: Influence of the binder chemistry

L. El Ouatani [a], R. Dedryvère [a,*], J.-B. Ledeuil [a], C. Siret [b], P. Biensan [b], J. Desbrières [a], D. Gonbeau [a]

[a] IPREM, Université de Pau, Hélioparc, 2 av. Pierre Angot, 64053 Pau Cedex 9, France
[b] SAFT, 111-113 bd. Alfred Daney, 33074 Bordeaux Cedex, France

ARTICLE INFO

Article history:
Received 24 July 2008
Received in revised form 15 October 2008
Accepted 7 November 2008
Available online 18 November 2008

Keywords:
Li-ion batteries
XPS
Graphite
SEI
CMC
SBR

ABSTRACT

We have investigated the possible effect of carboxymethylcellulose (CMC) in the SEI film formation at the surface of a graphite composite electrode of $LiCoO_2$/graphite cells. The electrode/electrolyte interface was analyzed by XPS at different potentials of the first electrochemical cycle, and after simple contact of the electrode with the electrolyte. We could evidence a specific reactivity of CMC towards the electrolyte ($LiPF_6$ in a mixture of carbonate solvents), resulting in the formation of new species that contribute to the surface film composition. This result shows that the chemical reactivity of CMC towards the electrolyte takes part in the formation of the surface film, and contributes to the good properties of CMC as binder.

1. Introduction

The high energy and power density of rechargeable lithium-ion cells make them attractive for a wide range of applications, from portable electronics to satellite applications. The even growing demand for energy storage requires further researches to improve the performance of this type of power source. Most commercial lithium-ion cells manufactured today consist of a carbon based negative electrode, a layered oxide positive electrode and an electrolyte based on a solution of a lithium salt in a mixture of organic solvents. Numerous researches have been carried out on electrode materials and electrolyte showing the importance of the choice of these components of the battery. Each electrode is obtained by depositing on a current collector a paste containing the electrochemically active material powder, conductive additives and a polymer binder mixed in water or in an organic solvent. The first purpose of using a polymer binder to prepare the electrode is to ensure cohesion of the active material particles. However, recent studies have shown that some binders used for the electrode preparation influence the electrochemical performances of the battery [1–4].

Generally, a good binder must meet different requirements. On the one hand, it must link active material particles together, allow the paste to adhere to the current collector and withstand the electrode volume change during the cycling of the cell; on the other hand it must be electrochemically stable and environmentally friendly.

The most common binder used in Li-ion batteries is poly(vinylidene fluoride) PVdF. The mechanical and electrochemical properties of PVdF are a good compromise between the multiple criteria described above. However, the stability of this binder towards reducing agents is not satisfactory because of the presence of fluorine, leading to safety problems in the event of thermal runaway [5]. Recently, many researches have been focused on another binder, namely carboxymethylcellulose sodium salt [4,6–12]. Its main advantage is to allow the preparation of the electrode in an aqueous solution, especially the graphite-based electrode.

Carboxymethylcellulose sodium salt (which will be called CMC in the following) is a derivative of cellulose consisting of a linear β-(1 → 4)-D-glucopyranose polymer, in which the —OH groups are partly substituted by $—OCH_2COO^-$, Na^+ groups. Because there are three —OH groups per monomer unit, the maximum degree of substitution (DS) is 3. The presence of the carboxymethyl groups is responsible for the aqueous solubility of CMC relative to insoluble cellulose. Therefore, CMC is a weak polyacid that dissociates to form carboxylate anion functional groups. The other predominant functional group on CMC is the hydroxyl.

It has been shown that CMC is an effective binder for the graphite negative electrode. A minimum content of 2 wt.% of CMC gives acceptable electrode properties, which is less than the conventional polymeric binders [4].

* Corresponding author. Tel.: +33 5 59 40 75 97; fax: +33 5 59 40 76 22.
E-mail address: remi.dedryvere@univ-pau.fr (R. Dedryvère).

0378-7753/$ – see front matter © 2008 Elsevier B.V. All rights reserved.
doi:10.1016/j.jpowsour.2008.11.031

Drofenik et al. [4] tested four different kinds of cellulose as binders in graphite electrodes and found that CMC shows the lowest irreversible loss in the first cycle and that its presence does affect neither the lithium intercalation/deintercalation nor the passivation processes thanks to the formation of a network around graphite particles rather than a compact film.

The effect of the DS of CMC on the dispersion properties of graphite in an aqueous medium was investigated by Lee et al. [7] It was found that suspension properties, as well as the quality of graphite particles dispersion, depend on the value of the DS. The analysis of the electrochemical performances of Li-ion batteries fabricated using aqueous formulations with different DS values showed better adhesion strength with a lower DS, and this appears to lead to longer cycle life with higher retention of discharge capacity during operational tests. Furthermore, the DS seems to also influence the energy density and specific capacity.

Lee et al. [6] have shown that the dispersion stability of a graphite suspension is improved when both Styrene Butadiene Rubber (SBR, an elastomeric copolymer of styrene and butadiene) and CMC are incorporated, compared with an unstable graphite suspension prepared with CMC alone. Graphite electrodes prepared in this way show improved electrochemical performances, with good rate capability and specific energy density.

CMC is also studied as a binder for non-carbonaceous alternative negative electrodes, especially silicon-based electrodes [8–11,13]. It has been shown to vastly improve the cycling performance and reversible capacity of Si-based electrodes [10]. The efficiency of this binder was attributed to its extended conformation in solution that facilitates a networking process of the conductive additive and Si particles during the composite electrode elaboration.

While the beneficial role of CMC on graphite electrode properties has been evidenced, the exact mechanisms are still not clear, despite the recent progress in understanding the role of this binder. Many fundamental questions are still open. Particularly, does CMC participate to the surface film formation? and what about its interaction with the active material and with the electrolyte?

In this paper, we investigate the role of CMC in a graphite composite electrode of $LiCoO_2$/graphite cells. The electrode/electrolyte interface was analyzed by X-ray photoelectron spectroscopy (XPS) at different potentials of the first electrochemical cycle, and after simple contact of the electrode with the electrolyte. For a better characterization of electrodes' surfaces, we present here an analysis of valence spectra coupled with a classical XPS core peaks investigation. Additional ^{1}H NMR spectroscopy and conductimetric titration experiments have been carried out to investigate the reactivity of CMC towards the electrolyte.

2. Experimental

2.1. Electrochemical measurements

Electrodes were provided by SAFT Research Department. The negative electrodes were prepared by depositing an aqueous mixture of 96% of graphite, and 4% of SBR and CMC as binders, on a copper foil current collector. The positive electrodes were prepared by coating an aluminum foil current collector with a slurry of 94% $LiCoO_2$, 4% poly(vinylidene fluoride) PVdF binder and 2% conductive carbon, in *N*-methyl-2-pyrrolidone. The electrodes were then dried at 120 °C for 12 h in an oven. The electrolyte was $LiPF_6$ 1 mol L^{-1} in a carbonate solvents mixture with a few % of VC (vinylene carbonate) additive.

Standard $LiCoO_2$/graphite coin-cells were assembled in a Jacomex argon dry box, in which the oxygen and water contents were maintained below 2 ppm, and then cycled at 20 °C using a Multichannel Potentiostat Galvanostat MPG testing apparatus (Bio-Logic SAS, Claix, France) performing under galvanostatic mode at C/20 rate. The first electrochemical cycle of the battery was stopped at the following potentials: 3.0, 3.8 and 4.2 V during charge, and 2.7 V during discharge. Each charge (or discharge) was followed by a floating step of 4 h, in which the voltage was maintained constant at the chosen value. Then, the positive and negative electrodes were carefully separated from the rest of the battery components in an argon dry box, washed with DMC solvent to remove the electrolyte, and dried prior to being packed into a hermetically sealed aluminum bag for transportation.

2.2. XPS

XPS measurements were carried out with a Kratos Axis Ultra spectrometer, using a focused monochromatized Al Kα radiation ($h\nu$ = 1486.6 eV). The XPS spectrometer was directly connected through a transfer chamber to a dry box, in order to avoid moisture/air exposure of the samples. For the Ag $3d_{5/2}$ line the full-width at half maximum (FWHM) was 0.58 eV under the recording conditions. The analyzed area of the samples was 300 μm × 700 μm. Peaks were recorded with a constant pass energy of 20 eV. The pressure in the analysis chamber was around 5×10^{-7} Pa. Short acquisition time spectra were recorded before and after each normal experiment to check that the samples did not suffer from degradation during the measurements. The binding energy scale was calibrated from the hydrocarbon contamination using the C 1s peak at 285.0 eV. Core peaks were analyzed using a nonlinear Shirley-type background [14]. The peak positions and areas were optimized by a weighted least-square fitting method using 70% Gaussian, 30% Lorentzian lineshapes. Quantification was performed on the basis of Scofield's relative sensitivity factors [15].

2.3. NMR

^{1}H NMR spectra were recorded at 25 °C in D_2O on a Bruker AVANCE 400 MHz spectrometer. All spectra were obtained at 400 MHz. Chemical shifts are reported in ppm and referenced to the TMS.

2.4. Conductimetric measurements

Conductimetric titration of CMC was carried out to determine its degree of substitution. It was performed using the back titration process. CMC was dissolved in water in which a 1 M NaOH solution was added to be sure that all carboxylic groups are ionized. Then the solution was titrated with a 5×10^{-3} M HCl solution using a CDM 230 conductimeter and a CDC-641 T conductivity cell from Radiometer Analytical.

3. Results and discussion

3.1. Study of the composite negative electrode

The first electrochemical cycle of the battery was stopped at the following potentials: 3.0, 3.8 and 4.2 V during charge, and 2.7 V during discharge, as shown in Fig. 1. The points (●) show the various samples studied *ex situ* by XPS. To complete this study, a negative electrode simply soaked for 4 h in the electrolyte and then washed with DMC was also analyzed.

Fig. 2 shows the evolution of C 1s, F 1s, P 2p core peaks and valence spectra of the composite negative electrode of these various samples. O 1s, Li 1s and Na 1s were also recorded but are not shown here for a non-exhaustive presentation. Results of quantitative analysis of these samples are reported in Table 1.

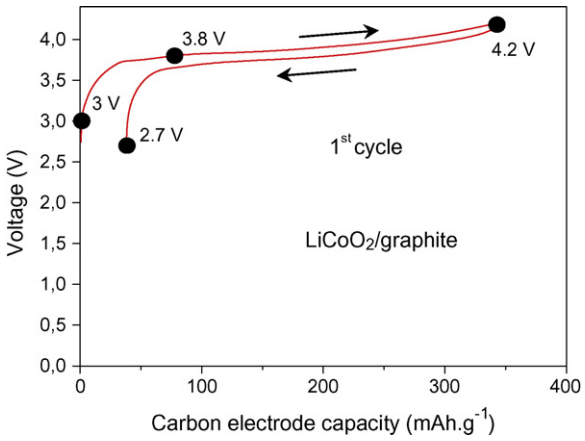

Fig. 1. First electrochemical cycle obtained at C/20 for the $LiCoO_2$/graphite cell. The samples studied *ex situ* by XPS are highlighted by points.

3.1.1. C 1s core peak

The C 1s spectrum of the composite electrode displays a narrow main peak at 284.2 eV assigned to graphite. The second peak at 285.0 eV is assigned to SBR binder (and also to hydrocarbon contamination), while the two other peaks observed at 286.7 and 288.4 eV are attributed to CO- and CO_2-like carbon atoms in the CMC binder, respectively.

The C 1s spectrum of the electrode simply soaked in the electrolyte shows a decrease of the graphite peak, suggesting that the formation of a passivating film at the surface of the negative electrode occurs as soon as it is in contact with the electrolyte, before the charge has started. In parallel with the diminution of the graphite peak, an increase of the 285 eV component is observed. This peak corresponds to C—C and C—H environments of carbon atoms, as found in hydrocarbon species.

Upon charge, we can observe a rapid decrease of the graphite component, showing that the active electrode material is being covered by a SEI film. The graphite component is hardly detectable at 3.8 V, which means that the SEI thickness is close to the analysis depth of XPS (about 5–10 nm). It is worth noting that O 1s spectra (Table 1) show in parallel the replacement of the O 1s components attributed to CMC by new components, thus showing that CMC is being covered by a surface film at the same time as graphite.

The C 1s spectra also display upon charge a strong increase of the 285 eV component with respect to the other components. Since this peak is attributed to the SBR binder in the fresh electrode, this observation may result from a covering effect of the CMC binder by a surface film at the same time as graphite that may not concern SBR. However, its increase is too important to be attributed only to this phenomenon. It is certainly also due to new hydrocarbon species resulting from degradation of CMC and/or solvent species (and to hydrocarbon contamination).

At the end of charge, other weak components can be observed:

- Two peaks at ~287 and 288.5 eV can be attributed to C—O and O═C—O environments of carbon, respectively. Since at this stage the CMC binder has been covered by a surface film, they can be attributed to new organic species formed in the SEI.
- Two peaks at ~289.8 and 291.3 eV can be assigned to different kinds of CO_3 environments. The former corresponds to lithium carbonate Li_2CO_3 and/or lithium alkyl carbonate $ROCO_2Li$ species resulting from the degradation of the solvent, while the latter can be attributed to VC-derived polymeric species [16]. Nevertheless, the amount of carbonate species remains very low. It is not so common to observe so few carbonates species according to the literature [17], however our observations are consistent with others studies [18–21].

After discharge at 2.7 V, the C 1s spectrum of the graphite electrode is very close to that obtained after the full charge (4.2 V). Particularly, the graphite peak still remains very weak, and the same components are observed. This suggests that the SEI is very stable and does not dissolve upon discharge.

3.1.2. F 1s core peak

The F 1s spectra of the same samples consist of two main peaks. The first one at ~685.2 eV is clearly attributed to LiF, which is a degradation product of $LiPF_6$ commonly observed at electrode/electrolyte interfaces. This peak is not observed after simple soaking of the electrode in the electrolyte. It appears at the beginning of charge, and its intensity increases at 4.2 V and remains stable upon discharge. The second peak at 687.1 eV can be assigned to the remaining salt $LiPF_6$, despite washing the electrode by DMC before XPS analysis. Moreover, an additional peak at ~689 eV was also observed, that could not be attributed.

Table 1
Binding energy (eV) and atomic percentage (%) of C, O, F, P, Li and Na elements of the complete composite electrode (graphite + SBR + CMC).

	Composite electrode		Soaked electrode		Charge 3 V		Charge 3.8 V		Charge 4.2 V		Discharge 2.7 V		Assignment
	BE (eV)	at.%	BE (eV)	at.%	BE (eV)	at.%	BE (eV)	at.%	BE (eV)	at.%	BE (eV)	at.%	
C 1s	284.2	22.2	284.4	11.5	283.9	5.7	282.8	1.5	282.7	1.2	283.6	2.4	Graphite
	285.0	42.9	285.0	36.8	285.0	36.3	285.0	39.8	285.0	30.9	285.0	37.4	C—C, C—H, C═C
	286.7	14.1	287.0	10.4	287.0	10.0	287.0	7.0	287.1	6.4	286.9	7.4	C—O
	288.4	3.0	288.6	1.1	288.5	1.9	288.7	1.9	288.3	1.6	288.4	1.6	COO
	–	–	289.8	0.9	289.4	0.9	289.8	1.8	289.6	1.9	289.6	1.7	CO_3(1)
	291.5	1.1	291.4	0.8	291.3	0.5	291.1	1.3	291.3	1.1	291.2	1.1	Sat. (C═C), CO_3(2)
O 1s	531.4	3.5	532.3	3.0	532.1	4.4	532.0	10.3	532.2	7.4	532.0	8.3	
	533.1	11.9	533.4	10.6	533.3	12.8	533.4	5.6	533.5	6.2	533.2	5.9	
	–	–	–	–	–	–	534.4	2.5	534.5	2.5	534.3	3.0	
F 1s	–	–	–	–	685.2	4.8	685.3	4.3	685.4	8.7	685.3	7.3	LiF
	–	–	686.9	16.2	687.1	10.8	687.1	9.3	687.2	15.3	687.0	9.8	$LiPF_6$, $Li_xPO_yF_z$
	–	–	688.8	2.0	688.9	2.2	689.1	1.1	688.9	0.8	689.0	0.8	
P $2p_{3/2}$	–	–	135.3	0.4	134.5	0.55	133.9	0.16	133.9	0.52	133.9	0.20	Phosphates
	–	–	–	–	135.4	0.74	135.0	0.36	135.2	0.65	135.2	0.85	$Li_xPO_yF_z$
	–	–	137.1	2.1	137.0	1.4	137.1	1.3	136.9	1.9	136.9	1.2	$LiPF_6$, Li_xPF_y
Li 1s	–	–	57.2	4.1	56.2	6.8	56.0	11.7	56.0	12.9	56.1	10.6	
Na 1s	1071.6	1.3	1072.8	0.1	1072.6	0.3	1072.7	0.08	1072.7	0.03	1072.5	0.45	

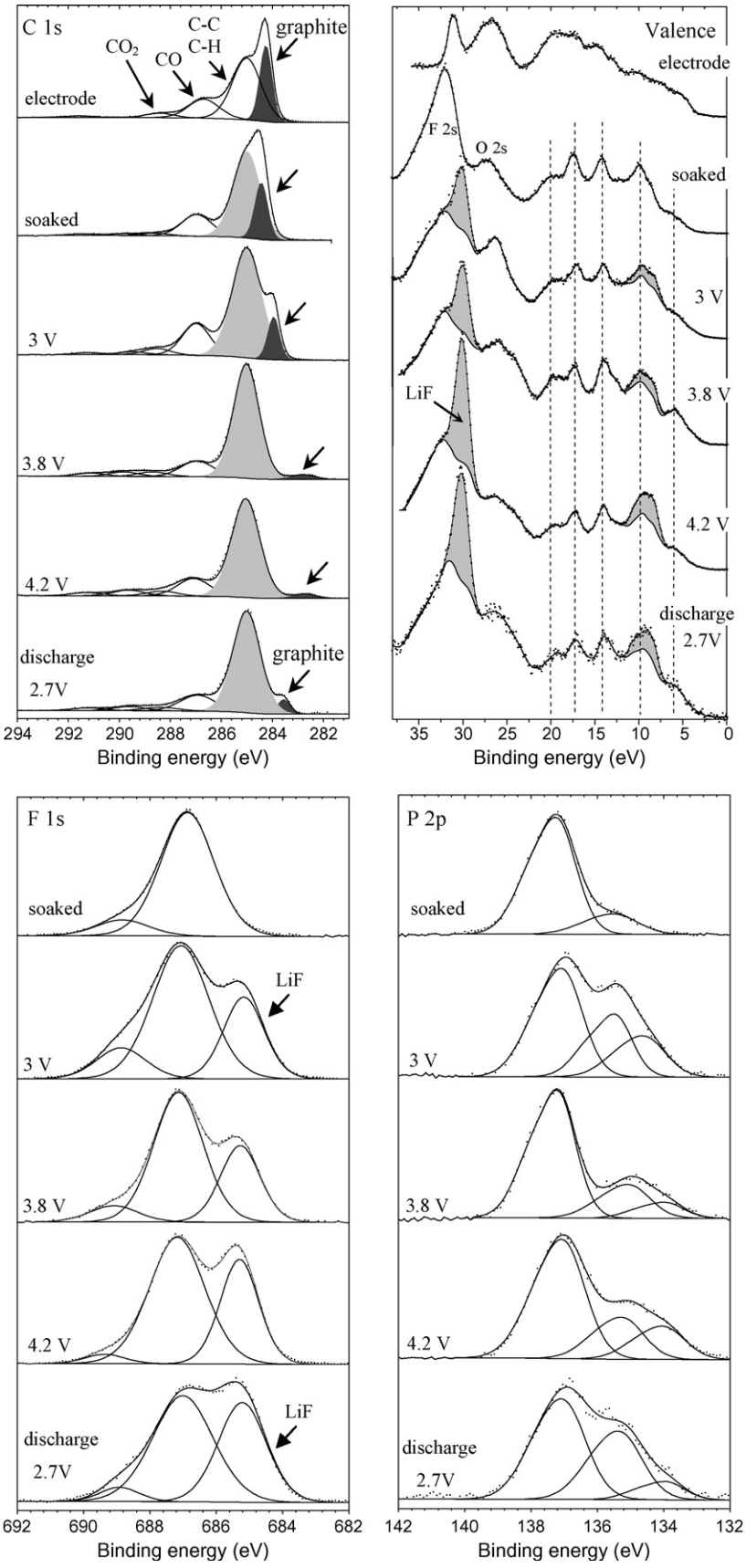

Fig. 2. C 1s, F 1s, P 2p core peaks and valence spectra of the composite negative electrode after soaking in the electrolyte, and at the various steps of the first cycle of the cell described in Fig. 1.

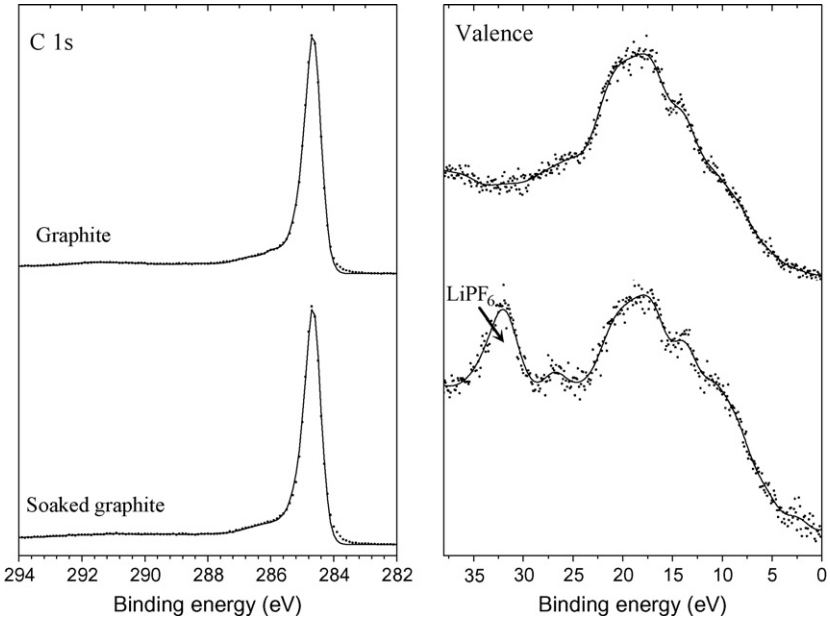

Fig. 3. C 1s core peak and valence spectrum of the graphite pellet electrode before and after soaking.

3.1.3. P 2p core peak

The P 2p spectra consist of several components (which are asymmetric doublets including $2p_{3/2}$ and $2p_{1/2}$ separated by ~0.9 eV). The first one at 137 eV can be attributed to the remaining salt $LiPF_6$. The two other ones at 134.1 and 135.3 eV can be assigned to phosphates and fluorophophates intermediates ($Li_xPO_yF_z$), respectively that result from degradation of $LiPF_6$. After simple soaking, the amount of degradation species is lower, and phosphates are not observed. No steady evolution of these species can be observed as a function of the potential.

As a summary, the analysis of XPS core peaks shows that the SEI is not only composed of organic species but also of inorganic compounds coming from the degradation of the salt. It shows that the SEI thickness increases upon charge and remains almost stable upon discharge.

3.1.4. Valence spectra

Additional information can be provided by the analysis of valence spectra of these electrodes. A clear interpretation of the valence spectrum of a complex mixture can be very difficult, since all the species present at the surface contribute to the valence spectrum. However, it can be simply used as a fingerprint of the surface chemistry, as its shape mainly results from the major species of the surface.

The valence spectrum of the composite electrode results from the mixture of graphite, CMC and SBR. The broad peak at 24–29 eV and the narrow peak at 31 eV are attributed to O 2s and Na 2p states from the CMC binder, respectively.

The valence spectrum of the electrode simply soaked in the electrolyte is completely changed: all the peaks are replaced by new ones. The maximum peak at 32 eV is attributed to F 2s states and is in good agreement with the appearance of fluorine at the surface (18 at.%), as shown in Table 1. This valence shape displays some similarities with the valence spectrum of the salt $LiPF_6$ [22]. However, the relative intensities of the peaks are not the same and additional peaks are present since this spectrum results from the complex mixture of the surface.

Upon charge and discharge, the amount of LiF increases, as shown previously. The valence spectrum of LiF consists in an intense narrow peak at 30 eV and a small peak at 8–10 eV. Therefore, for a better interpretation, the contribution of LiF has been subtracted from each valence spectrum (grey-filled areas), as shown in Fig. 2. This allows to evidence that the valence spectrum of the negative electrode does not significantly change upon charge and discharge, apart from the signature of LiF. Indeed, the same peaks with the same relative intensities can be observed over the first electrochemical cycle. Surprisingly, this particular shape appears as soon as the simple contact of the electrode with the electrolyte and is not significantly modified upon cycling. This observation lets us assume that a non-negligible part of the electrode/electrolyte interface results from the chemical reactivity of the electrode towards the electrolyte and is not due to the electrochemical reaction.

In order to better understand the origin of this reactivity, we decided to investigate each component of the negative electrode. Since the composite electrode is made up of graphite, and CMC and SBR as binders, we prepared the following negative electrodes to identify the role of each constituent: (1) a graphite pellet obtained by pressing the graphite powder at 4 tons cm^{-2} without binder, (2) a composite electrode made up of graphite and SBR (without CMC), and (3) a composite electrode made up of graphite and CMC (without SBR). For the two latter, the same preparation process as the complete composite electrode was used. These electrodes were soaked in the electrolyte for 4 h and then washed with DMC according to the same procedure and then analyzed by XPS. The obtained results are discussed below.

3.2. Graphite pellet

Fig. 3 shows the C 1s core peak and the valence spectrum of the graphite pellet electrode before and after soaking. The C 1s spectrum of the pristine sample displays the characteristic thin and asymmetric shape expected for graphite. After soaking, the C 1s spectrum does not practically change, showing that no carbonaceous species have formed at the surface of graphite. After soaking, F 1s and P 2p spectra (not shown here) reveal the presence of salt $LiPF_6$. The amount of LiF is very weak.

The valence spectrum of the pristine sample also displays the characteristic shape expected for graphite. After soaking, it does not significantly change, apart from the peak at 32 eV assigned to $LiPF_6$.

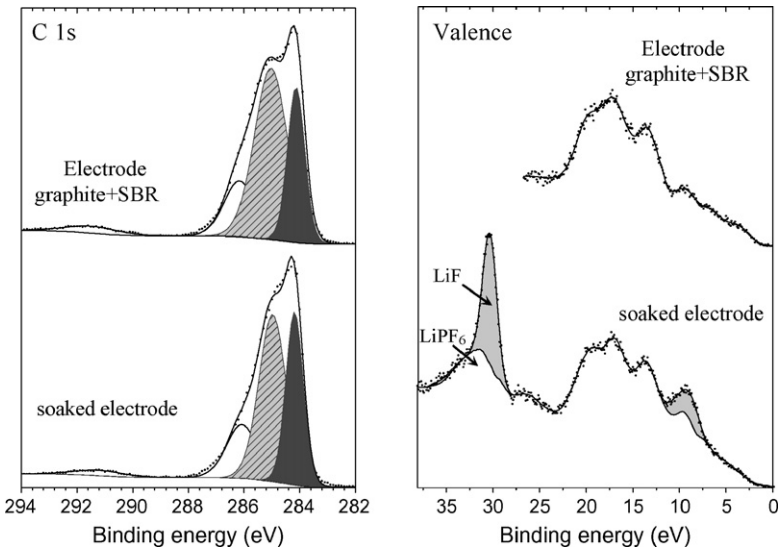

Fig. 4. C 1s core peak and valence spectrum of the graphite + SBR electrode (without CMC) before and after soaking in the electrolyte.

This analysis confirms that the chemical reactivity of graphite towards the electrolyte is very low, and that the active material of the electrode is not at the origin of the reactivity observed previously.

3.3. Graphite + SBR composite electrode

Fig. 4 shows the C 1s core peak and the valence spectrum of the composite electrode made up of graphite and SBR (without CMC).

The C 1s spectrum of the fresh electrode consists of two main peaks. The first one at 284.2 eV is attributed to graphite. The second one at 285 eV is attributed to C—C and C—H environments of carbon in SBR (and also to hydrocarbon contamination). An additional small peak at 286.2 eV results from electrode manufacturing, and the last peak at 291–292 eV is the "shake-up" satellite of graphite and SBR due to multielectronic transitions involving π–π^* transitions [23].

After soaking, the C 1s spectrum does not change, showing that no carbonaceous species have formed at the surface of this electrode. Besides, F 1s and P 2p spectra (not shown here) reveal the presence of LiF and small amounts of salt $LiPF_6$.

The valence spectrum of the fresh electrode results from the mixture of graphite and SBR. The four main components observed at 20, 17, 13 and 10 eV are characteristic of the C 2s molecular orbitals of aromatic rings in SBR [24]. After soaking, it does not significantly change, apart from the peaks at 30 and 32 eV assigned to LiF and $LiPF_6$, respectively. The same way as in Fig. 2, the contribution of LiF has been subtracted from the valence spectrum (grey-filled areas). These results show that the chemical reactivity of this graphite + SBR composite electrode towards the electrolyte is very low, and so that the SBR binder is not at the origin of the reactivity observed previously.

3.4. Graphite + CMC composite electrode

Contrary to the two previous samples, the mechanical properties of this composite electrode were good enough to carry out electrochemical experiments. Therefore, this electrode was not only soaked in the electrolyte. It was also used in $LiCoO_2$/graphite coin cells the same way as the complete composite electrode, and the electrochemical charge was carried out up to 4.2 V in the same conditions.

Table 2
Binding energy (eV) and atomic percentage (%) of C, O, F, P, Li and Na elements of the graphite + CMC electrode.

	Graphite + CMC electrode		Soaked electrode		Charge 3 V		Charge 3.8 V		Charge 4.2 V		Assignment
	BE (eV)	at.%	BE (eV)	at.%	BE (eV)	at.%	BE (eV)	at.%	BE (eV)	at.%	
C 1s	284.3	14.2	284.3	6.7	283.9	4.3	282.8	0.6	282.6	1.0	Graphite
	285.0	8.2	285.0	12.1	285.0	23.0	285.0	31.5	285.0	20.9	C—C, C—H, C=C
	286.9	29.2	286.9	18.7	287.1	15.9	287.0	10.1	287.0	8.8	C—O
	288.6	8.3	288.5	4.1	288.8	6.0	289.0	2.7	288.9	2.3	COO
	–	–	289.8	1.4	290.0	1.4	290.4	3.1	290.1	1.2	CO_3(1)
	–	–	–	–	291.1	0.6	291.1	0.7	291.1	0.6	CO_3(2)
O 1s	531.5	5.8	531.6	1.9	532.0	8.0	532.2	15.3	532.1	9.0	
	533.2	30.7	533.3	20.4	533.5	16.6	533.8	7.3	533.6	7.3	
F 1s	–	–	–	–	685.0	1.3	685.0	1.2	685.3	14	LiF
	–	–	686.8	24.2	687.2	13.8	687.2	14.7	687.2	12.7	$LiPF_6$, $Li_xPO_yF_z$
	–	–	688.8	2.7	–	–	–	–	–	–	
P $2p_{3/2}$	–	–	–	–	134.5	0.10	134.6	0.2	134.6	0.75	Phosphates
	–	–	135.0	0.27	–	–	–	–	–	–	$Li_xPO_yF_z$
	–	–	137.1	2.7	137.2	1.8	137.3	2.3	137.2	1.6	$LiPF_6$, Li_xPF_y
Li 1s	–	–	57.0	4.2	56.1	6.8	56.1	10.1	56.3	19.7	
Na 1s	1071.7	3.6	1072.5	0.6	1072.7	0.4	1072.8	0.2	1072.8	0.15	

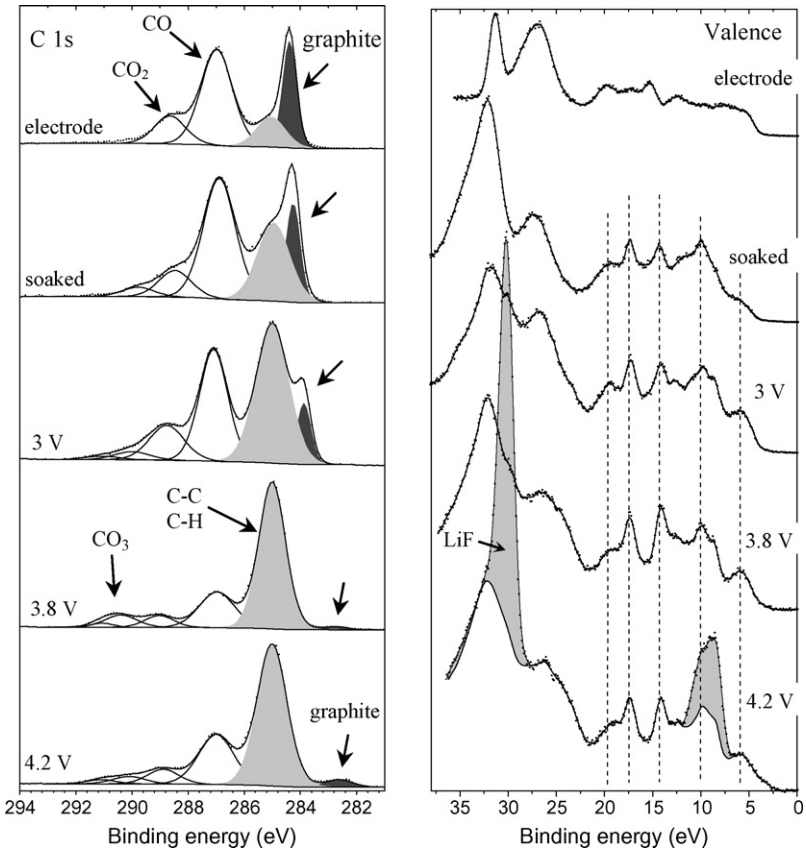

Fig. 5. C 1s core peaks and valence spectra of the fresh graphite + CMC electrode (without SBR), after soaking in the electrolyte, and after charge at 3.0, 3.8 and 4.2 V.

Fig. 5 shows the evolution of C 1s core peaks and valence spectra of the fresh graphite + CMC electrode, after soaking and after charge at 3.0, 3.8 and 4.2 V. Results of quantitative analysis of all elements are reported in Table 2.

3.4.1. C 1s core peak

The C 1s spectrum of the fresh electrode is composed of four peaks. The first one at 284.3 eV corresponds to graphite. The second one at 285 eV is assigned to hydrocarbon contamination. The last two peaks at 286.9 and 288.6 eV are respectively attributed to CO- and CO_2-carbon atoms of the CMC binder.

After soaking the graphite + CMC electrode in the electrolyte, it is important to note a decrease of the graphite peak, showing that the active electrode material has been covered by a film. In parallel with the diminution of the graphite peak, an increase of the 285 eV component is observed.

The C 1s spectrum of the soaked electrode also shows the appearance of a weak CO_3 component at 289.8 eV, suggesting the deposition of carbonate species at the electrode/electrolyte interface.

Upon charge, we can notice a progressive decrease of the graphite component at 284 eV, showing the continuous formation of the SEI at the surface of the electrode. This peak is hardly visible at the end of charge, which means that the SEI thickness is about 5–10 nm. We can also observe the increase of the 285 eV component and the formation of another carbonate component at 291 eV due to the formation of VC-derived polymeric species. We can notice at 3.8 V the enhancement of the other carbonate component at 289.8 eV, which can be due to the deposition of Li_2CO_3 and/or lithium alkyl carbonates $ROCO_2Li$. Note that the increase of the amount of carbonate species at the surface of the graphite electrode at this particular voltage (3.8 V) was already observed in a previous work [25].

Besides, F 1s and P 2p spectra (not shown here) reveal the presence of LiF, $LiPF_6$, phosphates and fluorophosphates intermediates, as shown above for the complete composite electrode.

3.4.2. Valence spectra

The valence spectrum of the fresh electrode is very close to that of pure CMC. The broad peak at 24–29 eV and the narrow peak at 31 eV are attributed to O 2s and Na 2p states.

After soaking, the valence spectrum is completely changed. It is almost identical to that obtained for the complete composite electrode in the same conditions, showing that the composition of the surface is almost the same. Moreover, the same way as for the complete composite electrode, the valence spectrum does not significantly change upon charge, apart from the signature of LiF at 4.2 V (grey-filled areas). Therefore, we can conclude again that a non-negligible part of the surface composition results from the chemical reactivity of the electrode towards the electrolyte and is not due to the electrochemical reaction. Since this reactivity can be attributed neither to graphite nor to SBR, this is an evidence of the chemical reactivity of CMC towards the electrolyte.

In order to investigate whether this reactivity affects the C—C bonds of CMC, we carried out ^{1}H NMR measurements on CMC before and after contact with the electrolyte. With this aim, the CMC binder was soaked for 4 h in the electrolyte and then washed with DMC to remove the salt. Pristine and soaked CMC were then dissolved in D_2O and analyzed by ^{1}H NMR. D_2O was chosen as solvent for this analysis because CMC has a very poor solubility in common organic solvents. Obviously, this choice of solvent may mask some part of the information, since organic functions resulting from the reactivity of CMC towards the electrolyte in aprotic medium may be hydrolyzed in water. However, if important changes in the molecular structure of CMC occur during contact with the electrolyte (as

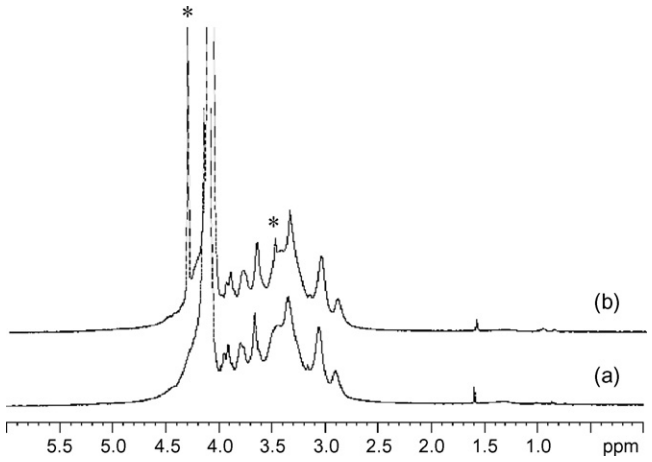

Fig. 6. ^{1}H NMR spectra of: (a) CMC and (b) CMC soaked in the electrolyte (*peaks due to remaining traces of electrolyte).

for example breaking of C—C bonds), it should be detected in the ^{1}H NMR spectra despite this contact with D_2O. The obtained results are shown in Fig. 6. The spectra of the two samples are identical, apart from two peaks at 3.5 and 4.3 ppm which are attributed to the remaining electrolyte despite washing the soaked sample with DMC (as demonstrated from the NMR spectrum of the electrolyte in the same analysis conditions). This result shows either that the structure of CMC is not modified after contact with the electrolyte, or that these modifications concern only its extreme surface (since NMR provides a characterization of the bulk sample).

Additional information was provided by conductimetric titration of CMC in order to determine its degree of substitution. The obtained results were the same before and after contact with the electrolyte. In this experiment too, CMC was dissolved in aqueous solution, however this result allows to show that the DS of the bulk CMC did not change after contact with the electrolyte, which is in agreement with NMR analyses.

Concerning a possible change of the DS at the extreme surface of CMC, further interpretation of C 1s spectra of the graphite + CMC electrode shown in Fig. 5 may provide additional information. Indeed, the 286.9 eV component is a signature of CO-like carbon atoms of CMC, while the 288.6 eV component is a signature of CO_2-like carbon atoms. The amount of CO_2-like carbon atoms may vary if the DS of CMC changes at the surface after contact with the electrolyte. On the other hand, the amount of CO-like carbon atoms is expected to be stable. Moreover, after soaking, these two C 1s components are still exploitable since the amount of deposited carbonaceous species is weak.

In the fresh electrode, the Na/C_{CO} ratio is 0.12, while in the soaked electrode the Na/C_{CO} ratio is only 0.03. Therefore, after simple contact of CMC with the electrolyte, the amount of sodium has been divided by 4. This loss of sodium could be due to a decrease of the DS of CMC following its reactivity towards the electrolyte. However, in the same time, the CO_2/CO ratio changes from 0.28 to 0.22, which is not significant. As a result, the loss of sodium induced by soaking the electrode in the electrolyte cannot be attributed to a decrease of the DS of CMC at the surface. It is more likely explained by an exchange between Li^+ and Na^+ ions in the ($—CH_2COO^-$, Na^+) functional group of CMC.

Therefore, we can assume that the reactivity of CMC towards the electrolyte may be due to the other functional groups of CMC at the surface, *i.e.* hydroxyl groups —OH, which are very numerous. While the reactivity of CMC in an aqueous medium is well known, very few data are available concerning its reactivity in a complex organic medium such as the electrolyte used in this work. A precise interpretation of the particular valence spectrum shape that was evidenced for electrodes containing CMC was not possible, certainly because it corresponds to a complex mixture of compounds. However, some similarities with the valence spectrum of $LiPF_6$, as well as significant amounts of phosphorus and fluorine at the surface of the electrode when CMC is used as binder, let us assume that CMC may react with the salt. Considering the reactivity of $LiPF_6$, we can advance some hypotheses. Indeed, even at room temperature the following equilibrium produces PF_5, a strong Lewis acid [17]:

$$LiPF_6 \leftrightarrow LiF + PF_5 \quad (1)$$

Therefore, PF_5 may react with the —OH groups of CMC, leading to the following overall mechanism:

$$R\text{–}OH + LiPF_6 \rightarrow R\text{–}O\text{–}PF_4 + LiF + HF \quad (2)$$

thus resulting in $–PF_4$ groups grafted at the surface of the CMC binder. This could explain why we systematically observe this particular valence spectrum which resembles that of $LiPF_6$, but cannot be attributed only to the salt.

Another important result has to be explained. Upon cycling, C 1s spectra are dominated by the strong increase of the 285 eV component (Figs. 2 and 5). As said above, this component is attributed to C—C and C—H environments of carbon atoms, as found in hydrocarbon species. This phenomenon is not necessarily due to the CMC binder. Indeed, Peled and coworkers already observed such an intense XPS peak at the surface of carbonaceous electrodes, that they assigned to the formation of polyolefines [26]. Besides, Novák and coworkers have shown by using *in situ* differential electrochemical mass spectroscopy the formation of ethylene gas during the first charge of graphite in an EC/DMC based electrolyte [27,28]. Moreover, Endo et al. [29] have shown that the reductive electrolysis of ester-based electrolyte solutions results in a continuous production of alkyl radicals. They suggested that these radicals can initiate a chain reaction leading to polymers. Aurbach et al. already proposed the formation of polyethylene at the surface of a graphite electrode [30]. We can thus assume that polymerisation of ethylene gas may occur during the first cycle, which may explain the origin of this 285 eV component.

4. Conclusion

In this work, we have studied the formation of the SEI at the surface of a graphite negative electrode. We have investigated the role of each component of the electrode: the graphite active material, the CMC and SBR binders. We observed a very stable SEI, with a very low content of carbonate species. From a detailed analysis of XPS data, particularly valence spectra, we could evidence a specific reactivity of CMC towards the electrolyte, resulting in the formation of new species after simple contact of the electrode with the electrolyte, that do not disappear upon electrochemical cycling and constitute a non-negligible part of the surface composition. This result shows that the chemical reactivity of CMC towards the electrolyte, probably due to hydroxyl groups at the surface, takes part in the formation of the surface film. This reactivity may contribute to the beneficial role of CMC with respect to irreversible capacity of a graphite electrode in the first cycle.

Acknowledgments

We thank French CNRS (National Center for Scientific Research) and Region Aquitaine for financial support.

References

[1] L. Fransson, T. Eriksson, K. Edström, T. Gustafsson, J.O. Thomas, J. Power Sources 101 (2001) 1.
[2] M.N. Richard, J.R. Dahn, J. Power Sources 83 (1999) 71.

[3] M. Gaberscek, M. Bele, J. Drofenik, R. Dominko, S. Pejovnik, Electrochem. Solid-State Lett. 3 (2000) 171.
[4] J. Drofenik, M. Gaberscek, R. Dominko, F.W. Poulsen, M. Mogensen, S. Pejovnik, J. Jamnik, Electrochim. Acta 48 (2003) 883.
[5] P. Biensan, B. Simon, J.P. Pérès, A. de Guibert, M. Broussely, J.M. Bodet, F. Perton, J. Power Sources 81–82 (1999) 906.
[6] J.-H. Lee, S. Lee, U. Paik, Y.-M. Choi, J. Power Sources 147 (2005) 249.
[7] J.-H. Lee, U. Paik, V.A. Hackley, Y.-M. Choi, J. Electrochem. Soc. 152 (2005) A1763.
[8] W.-R. Liu, M.-H. Yang, H.-C. Wu, S.M. Chiao, N.-L. Wu, Electrochem. Solid-State Lett. 8 (2005) A100.
[9] H. Buqa, M. Holzapfel, F. Krumeich, C. Veit, P. Novak, J. Power Sources 161 (2006) 617.
[10] B. Lestriez, S. Bahri, I. Sandu, L. Roue, D. Guyomard, Electrochem. Commun. 9 (2007) 2801.
[11] J. Li, R.B. Lewis, J.R. Dahn, Electrochem. Solid-State Lett. 10 (2007) A17.
[12] S. Barusseau, F. Martin, B. Simon, US Patent 6,183,907 (2001).
[13] N.S. Hochgatterer, M.R. Schweiger, S. Koller, P.R. Raimann, T. Wohrle, C. Wurm, M. Winter, Electrochem. Solid-State Lett. 11 (2008) A76.
[14] D.A. Shirley, Phys. Rev. B 5 (1972) 4709.
[15] J.H. Scofield, J. Electron Spectrosc. Relat. Phenom. 8 (1976) 129–137.
[16] L. El Ouatani, R. Dedryvère, C. Siret, P. Biensan, S. Reynaud, P. Iratçabal, D. Gonbeau, J. Electrochem. Soc., 156 (2009) in press.
[17] K. Xu, Chem. Rev. 104 (2004) 4303.
[18] G.V. Zhuang, J. Ross, N. Philip, Electrochem. Solid-State Lett. 6 (2003) A136.
[19] S. Verdier, L. El Ouatani, R. Dedryvere, F. Bonhomme, P. Biensan, D. Gonbeau, J. Electrochem. Soc. 154 (2007) A1088.
[20] V. Eshkenazi, E. Peled, L. Burstein, D. Golodnitsky, Solid State Ionics 170 (2004) 83.
[21] K. Edström, M. Herstedt, D.P. Abraham, J. Power Sources 153 (2006) 380.
[22] R. Dedryvère, S. Leroy, H. Martinez, F. Blanchard, D. Lemordant, D. Gonbeau, J. Phys. Chem. B 110 (2006) 12986–12992.
[23] D. Briggs, M.P. Seah, in: D. Briggs (Ed.), Practical Surface Analysis by Auger and X-ray Photoelectron Spectroscopy, John Wiley and Sons, 1983.
[24] J.P. Boutique, J. Riga, J.J. Verbist, J. Delhalle, J.G. Fripiat, J. Electron Spectrosc. Relat. Phenom. 33 (1984) 243–262.
[25] S. Leroy, F. Blanchard, R. Dedryvère, H. Martinez, B. Carré, D. Lemordant, D. Gonbeau, Surf. Interf. Anal. 37 (2005) 773–781.
[26] V. Eshkenazi, E. Peled, L. Burstein, D. Golodnitsky, Solid State Ionics 170 (2004) 83–91.
[27] P. Novák, F. Joho, R. Imhof, J.-C. Panitz, O. Haas, J. Power Sources 81–82 (1999) 212.
[28] M. Lanz, P. Novák, J. Power Sources 102 (2001) 277.
[29] E. Endo, M. Ata, K. Sekai, K. Tanaka, J. Electrochem. Soc. 146 (1999) 49–53.
[30] D. Aurbach, B. Markovsky, I. Weissman, E. Levi, Y. Ein-Eli, Electrochim. Acta 45 (1999) 67.